Analog Programmable-Photonic Computation

Andrés Macho-Ortiz, Daniel Pérez-López, José Azaña, and José Capmany**

Digital electronics is a technological cornerstone in this modern society that has covered the increasing demand for computing power during the last decades thanks to a periodic doubling of transistor density in integrated circuits. Currently, such scaling law is reaching its fundamental limit, leading to the emergence of a large gamut of applications that cannot be supported by digital electronics, specifically, those that involve real-time multi-data processing, e.g., medical diagnostic imaging, robotic control, and autonomous driving, among others. In this scenario, an analog computing approach implemented in a real-time reconfigurable nonelectronic hardware such as programmable integrated photonics (PIP) can be more efficient than digital electronics to perform these emerging applications. However, actual analog computing models such as quantum and neuromorphic computation were not conceived to extract the unique benefits of PIP (and integrated photonics in general). Here, the foundations of a new computation theory are presented, termed Analog Programmable-Photonic Computation (APC), explicitly designed to unleash the full potential of PIP technology. Interestingly, APC enables overcoming basic theoretical and technological limitations of existing computational models and can be implemented in other technologies (e.g., in electronics, acoustics or using metamaterials), consequently exhibiting the potential to spark a ground-breaking impact on the information society.

1. Introduction

Over the last decades, digital electronic technology has supported the increasing demand for computing power thanks to an exponential performance scaling in microelectronics. In particular, this progress is embodied in Moore's and Dennard's laws by which the density of transistors, power efficiency, and clock frequency in microprocessors has approximately doubled every 18–24 months.[1,2] Nevertheless, as seen in **Figure 1**a, these scaling laws are reaching their fundamental limits. As a result, there is currently a wide range of emerging realtime signal processing and computing applications (including medical diagnostic imaging, robotic control, remote sensing, smart homes, drug design, and autonomous driving, among others) that may not be efficiently dealt with using the dominant digital electronic paradigm.[1–6]

Despite the fact that the electronic industry has proposed to circumvent the end of Moore's and Dennard's laws by introducing multi-core technology, there is a limit in the number of cores that can simultaneously be powered on with a fixed power budget and a constant heat extraction rate (Amdahl's law).[2,3] Moreover, as the bandwidth limitations of silicon electronics and printed metallic tracks are reached, the power consumed in data transport in an electrical circuit cannot be further reduced.[2,4] These physical bottlenecks – in combination with the fact that conventional computational models are conceived as serialized and centralized processing architectures (von-Neumann machines) implementing the nonlinear Boolean algebra – severely limit the performance of digital electronic computers.[1,2,7–9] In general, such schemes are inefficient in performing multi-linear operations and computational architectures that are distributed, parallel, and adaptive (Figure 1b); for instance, those used to perform real-time matrix operations, requiring high bandwidth, low energy consumption, and high reconfigurability (such as the applications mentioned above).[5,6]

Although from the Church–Turing thesis, it can be inferred that any class of computational problem (or computable function) can be solved by a digital electronic computer,[2,10] this does not imply that digital computation.[9] and electronic technology always lead to the most suitable marriage between a mathematical computing theory and a hardware platform. Analog computing approaches implemented in alternative system-on-chip

A. Macho-Ortiz, D. Pérez-López, J. Capmany
ITEAM Research Institute
Universitat Politècnica de València
Valencia 46022, Spain
E-mail: amachor@iteam.upv.es; jcapmany@iteam.upv.es

D. Pérez-López, J. Capmany
iPronics
Programmable Photonics
S.L
Camino de Vera s/n
Valencia 46022, Spain

J. Azaña
Institut National de la Recherche Scientifique – Énergie
Matériaux
et Télécommunications (INRS-EMT)
Montréal, QC Canada

The ORCID identification number(s) for the author(s) of this article can be found under https://doi.org/10.1002/lpor.202200360

DOI: 10.1002/lpor.202200360

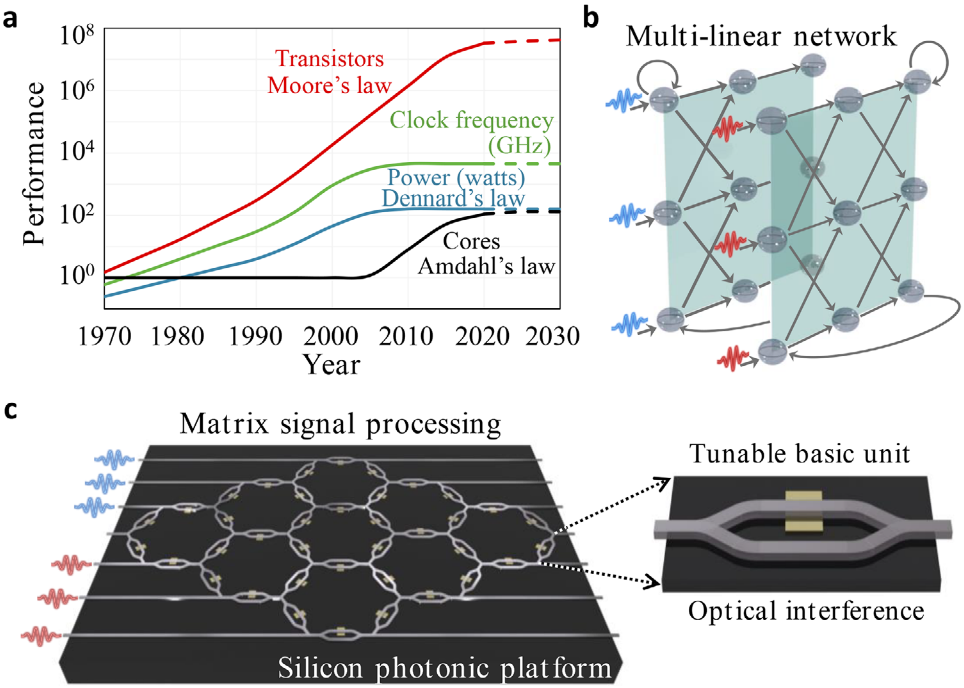

Figure 1. Limitations of digital electronics and complementary system-on-chip technology. a) Historical evolution and perspective of the main performance parameters of digital electronics.[3] b) Distributed, parallel, and adaptive computational network performing multi-linear operations via real-time matrix transformations of the input signals, a scenario where digital electronic paradigm shows significant mathematical and technological limitations.[5,6] c) Programmable integrated photonic circuit integrated into a silicon photonic platform. This hardware technology can be co-integrated with microelectronic processors to carry out parallel reconfigurable matrix transformations on the input signals using optical interference as a fundamental physical principle.[12–14].

technologies can be mathematically more efficient than digital computation in solving the aforementioned computational scenarios and may provide hardware advantages over electronics in basic performance parameters (bandwidth, parallelism, power consumption, or reconfigurability).[1,5,6,10,11] Specifically, technologies that are inherently capable of performing matrix operations offering complementary hardware requirements to those of electronics and being CMOS-compatible are a priority.[1,4,12–14]

In this context, a new hardware technology has emerged in recent years: programmable integrated photonics (PIP).[12–14] PIP is a system-on-chip platform that enables the programming of advanced signal processing tasks by leveraging on the capacity of integrated photonic circuits to manage multiple optical interferences. In essence, this entails the independent setting of amplitude and phase characteristics of interfering signals by employing meshes of tunable basic units (i.e., basic building blocks) that are constructed from mainstream integrated optical devices: phase shifters, beam splitters, beam combiners, and resonators.[14–16] The combination and interconnection of such devices allow the implementation of PIP circuitry featuring various degrees of complexity and functionality, which can be grouped into three families:[13] application-specific photonic integrated circuits, multi-port interferometers, and photonic waveguide meshes.

PIP is the ideal hardware technology to explore an analog computing paradigm for a variety of reasons. First, PIP is able to carry out reconfigurable matrix transformations on the input waves by programming the transfer matrix of the PIP platform via external electrical signals (Figure 1c). Second, PIP circuits can be co-integrated with microelectronic processors by exploiting its CMOS compatibility via compact silicon photonic platforms with complementary features to electronics: high bandwidth, massive parallelism via wavelength-division multiplexing, low power consumption, and high reconfigurability.[12–14] This combination of characteristics cannot concurrently be found in other optical platforms based on metamaterials,[17,18] photonic crystals,[19,20] nanowire networks,[21] plasmonic waveguides,[22,23] free-space optics,[5] and nonlinear optics.[4,24,25] Third, PIP benefits from the scalable fabrication methods of integrated circuits and its manufacturing could achieve economies of scale comparable with the microelectronic industry in the next decades.[12]

So far, PIP has essentially been explored as a hardware-accelerated solution for existing computational models such as digital,[9] quantum,[10] and neuromorphic computation[26] implemented in electronic circuits. Here, PIP only carries out signal processing tasks (i.e., wave transformations), which involve a high degree of complexity in electronics, in particular, multi-dimensional wave transformations via vector-by-matrix multiplications.[12–14,27] Nonetheless, PIP has not yet been utilized to perform true computational tasks, i.e., transformations of units of information. A unit of information is the basic mathematical object of any computation theory where user information is encoded to be transformed by mathematical functions termed computational operations or gates (e.g., in electronics the computational tasks are Boolean operations on digital bits, which

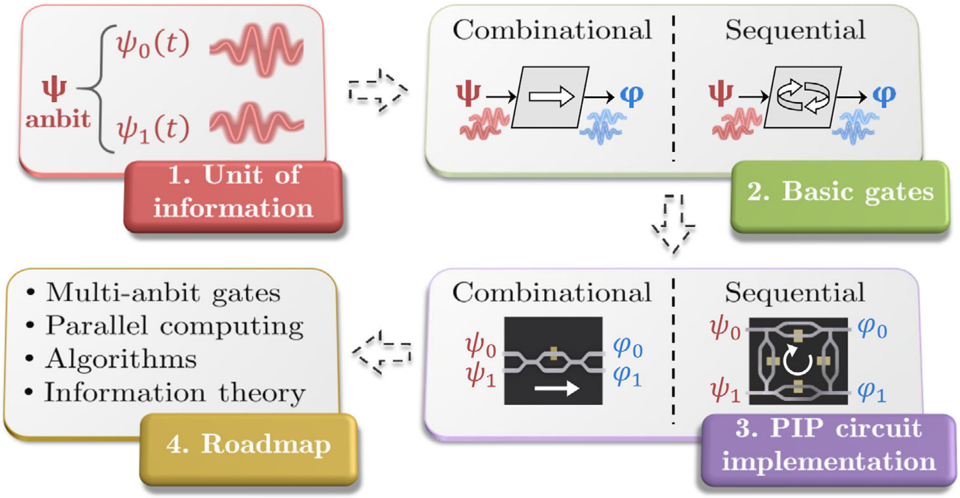

Figure 2. Construction of the computation theory proposed in this work. Flowchart of the steps required to construct the new computing model, termed Analog Programmable-Photonic Computation (APC), implementable with programmable integrated photonic (PIP) technology. APC revolves around the idea of performing operations on a new unit of information, the analog bit or anbit (Step 1), evolving the concept of optical signal processing shown in Figure 1c into true optical computing. The computational operations (or gates) are classified in two main classes: combinational and sequential systems (Step 2), which are respectively implemented by using non-feedback and feedback PIP circuits (Step 3). Note that the circuits shown in Step 3 are only illustrative schemes of non-feedback and feedback PIP configurations. The specific circuitry of combinational and sequential systems is sketched in Figure 5 and Figure 7. Finally, a roadmap details the additional concepts that should be developed in future research to extend the fundamental principles of the computational framework presented in this work (Step 4).

respectively constitute the gates and the units of information in digital computation.[9])

In fact, at present, there is no specific computation theory available – explicitly designed for PIP (and integrated photonics in general) – that allows us to exploit this technology to implement true optical computing, in the same way as digital computation sparked a paradigm shift in electronics. Moreover, digital, quantum, and neuromorphic computation were not conceived to extract the whole benefits of PIP since these models were originally built without considering the complexity of their implementation in integrated optics.[4,6,11,28–30]

Being PIP a hardware technology that naturally performs matrix transformations on optical signals, and whose building block may be designed by using a mathematical framework similar to quantum computing[31] (based on matrix transformations of the quantum bits or qubits, which are respectively the gates and the units of information in quantum computation), one could ask whether a classical version of quantum computing might be proposed within the realm of classical wave-optics. Different attempts have been reported revolving around this idea in order to:[32–40] (i) simulate a quantum computer with a classical computer and (*ii*) dig into the fundamental differences between quantum and classical systems. However, to our knowledge, the quantum computing formalism has never been extrapolated to a classical scenario to construct an analog computing landscape based on deterministic physical laws. This would offer a novel computational framework that could allow us to realize two significant goals. First, harness the full potential of PIP technology by designing a computing model (unit of information and gates) with mathematical properties matched to the ability of PIP to carry out vector-by-matrix multiplications. Second, overcome some of the basic theoretical and technological limitations of quantum computing, such as the need to operate with extremely low temperatures, the practical difficulties of scaling the capabilities of a quantum computer to a large number of qubits, the wave function collapse in data measurement, and the impossibility of performing cloning, summation, and feedback operations.[10,34,41,42]

To this end, here we present the foundations of an entirely new class of computation theory, termed Analog Programmable-Photonic Computation (APC). To achieve this overall aim, we will follow the steps sketched in **Figure 2**. First, we will propose a unit of information named as **analog bit** (or anbit), defined as a 2D analog vector function (similar to the qubit, but with essential differences, as detailed below). Second, we will introduce the basic **computational operations** (anbit gates), based on matrix algebra. Third, we will design the **circuit implementations** of these gates using PIP technology. Fourth, we will specify the class of **computational problems** that can be handled with APC (including some basic examples and applications) and a roadmap to further develop this computational model in future research. Finally, a qualitative comparison among the **main properties** of APC versus digital, quantum, and neuromorphic computation is discussed, assessing the unique potential and versatility offered by this new computing paradigm.

2. Preliminary Concepts on Information Processing

Before delving into the theory of any computational model, it is helpful to first describe how the user information is processed from an information-theoretical approach. This entails having a perspective of any computational architecture (classical or quantum and digital or analog) as a communication system composed by a transmitter, a channel, and a receiver where information is respectively generated, propagated, and recovered (**Figure 3**).[43,44]

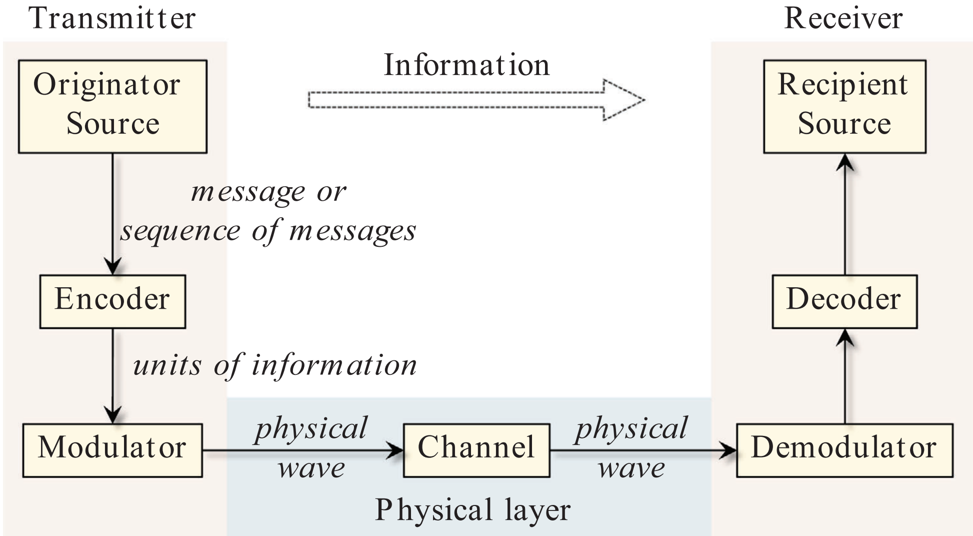

Figure 3. Block diagram of a generic communication system. Any computational architecture (classical or quantum and digital or analog) can be regarded as a communication system composed by a transmitter where information is generated, a channel where information is propagated (e.g., the circuits of an optical chip), and a receiver where information is recovered.[43,44] In the first (mechanical and electronic) analogue computers, the encoder and modulator are implemented by a single block that directly maps the information of the originator source into a physical wave.[18] Such a mapping is traditionally termed as an "analogy". At the receiver, the demodulator and decoder are also implemented by a single block that reverses the analogy. In contrast, in modern analog computing models (such as quantum computation and APC), the encoder (decoder) and modulator (demodulator) are usually independent blocks.

Concretely, the transmitter is composed by three subsystems. First, an originator source that generates a single message (e.g., an image) or a sequence of messages (e.g., a sequence of letters).[45] The kind of messages generated by the originator source may be the same in digital, quantum, and neuromorphic computing,[43–47] as well as in APC.

Second, an encoder that maps this information into a "container" of information commonly termed as **unit of information** (but not in the strict sense of physical unit since such a container of information may encode a variable amount of information, e.g., as can be observed in the qubit via the Holevo bound.[44]) Bearing in mind both classical and quantum information theories,[43,44] a unit of information can be defined in a unified way as a time-dependent function that may be continuous or discrete in time and with values belonging to a continuous- or discrete-state space (in the discrete-time case, the output of the encoder is usually modeled as a sequence of units of information given that each time interval can be regarded as a different unit of information). Specifically, we deal with a digital computation theory when the unit of information is a discrete-time function with values belonging to the discrete-state space $\{0,1\}$ (the digital bit).[43] Otherwise, we deal with an analog computation theory, where the unit of information is defined as a continuous- or discrete-time function with values ranging on a continuous- or discrete-state space (but different from $\{0,1\}$).[44,48–50]

Third, a modulator that converts the units of information into physical (electromagnetic, acoustic, or mechanical) waves that will be propagated through the channel. Such a mapping is known as modulation format.[43] In a computational system, the channel propagates and transforms the physical waves encoding the units of information to carry out a series of computational operations required to solve a specific mathematical problem.

Finally, the receiver restitutes the information by means of a demodulator that transforms the physical waves into units of information, a decoder mapping the units of information into a message (or a sequence of messages), and a recipient source providing an interpretation of such information.

In particular, APC is a computing model that will be implemented in a PIP platform to solve mathematical problems that are inefficiently handled by digital electronics. This implies that any APC architecture can be regarded as a communication system where integrated electronic and photonic circuits should coexist. Whilst the originator (recipient) source and the encoder (decoder) will be implemented with integrated electronics, the modulator (demodulator) and the channel will be carried out within the realm of integrated photonics. The bridge between both system-on-chip technologies is performed by an electro-optic (opto-electrical) conversion at the modulator (demodulator).

From these preliminary concepts of information processing, it can be inferred that the design of the unit of information is vital to endow a computational model with the sought-after properties. Outstandingly, in our case, APC will be devised as a versatile **analog computing paradigm** matched to current and future PIP technology via a unit of information that can be deemed as a discrete- or continuous-time function.

3. Unit of Information: the Analog Bit

APC revolves around the idea of performing operations on a new unit of information, the **anbit**, which must be easily

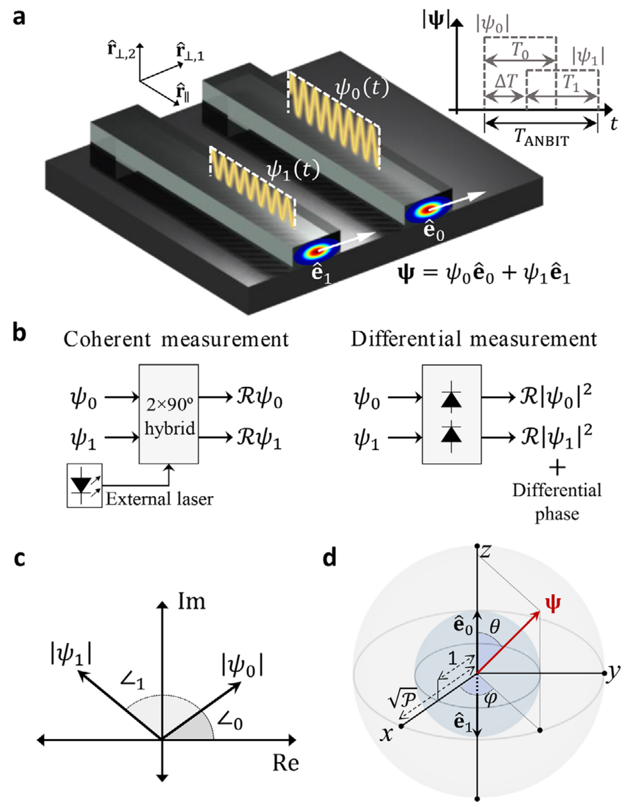

Figure 4. The analog bit. a) Physical implementation of an anbit $\boldsymbol{\psi}(t) = \psi_0(t)\hat{e}_0 + \psi_1(t)\hat{e}_1$ using PIP technology and space-anbit modulation (see Methods). The anbit amplitudes $\psi_{0,1} = |\psi_{0,1}|\, e^{i\angle_{0,1}}$ are mapped onto two optical wave packets propagated by the fundamental modes $\hat{e}_{0,1}$ of two uncoupled waveguides. b) Different classes of anbit measurement using coherent or direct detection. In the former case, an anbit of the form $\mathcal{R}\psi_0\hat{e}_0 + \mathcal{R}\psi_1\hat{e}_1$ is measured, where $\mathcal{R}$ is the responsivity of the photodiodes of a 90-degree hybrid architecture. In the latter case, an anbit of the form $\mathcal{R}|\psi_0|^2\hat{e}_0 + \mathcal{R}|\psi_1|^2 e^{i(\angle_1-\angle_0)}\hat{e}_1$ is retrieved (see Section S1.2, Supporting Information for more details). c) Geometric representation of an anbit with 4 effective degrees of freedom (EDFs) using a polar diagram in the complex plane. d) Geometric representation of an anbit with 3 EDFs in the generalized Bloch sphere (GBS). Here, the anbit $\boldsymbol{\psi}$ can equivalently be written as $\boldsymbol{\psi} = \sqrt{\mathcal{P}}\,(\cos(\theta/2)\hat{e}_0 + e^{i\varphi}\sin(\theta/2)\hat{e}_1)$, see Section S1.3, Supporting Information.

implementable using PIP technology. Since the building block of PIP is usually an optical circuit carrying out 2×2 matrix transformations,[12–14,31] the input and output signals of this system are 2D vectors. Thus, it seems reasonable to define an anbit as a 2D vector function $\boldsymbol{\psi}(t) := \psi_0(t)\mathbf{e}_0 + \psi_1(t)\mathbf{e}_1$, where $\psi_{0,1}$ are scalar complex functions referred to as the anbit amplitudes and $\mathbf{e}_{0,1}$ are constant orthonormal vectors. The anbit amplitudes can take on a continuous range of **complex values** and should be conceived as discrete-time functions to be fitted to the technological features of present PIP platforms, implementing matrix transformations that are reconfigurable in time, but with constant matrix entries when the signals are propagated through the circuits. Accordingly, $\boldsymbol{\psi}$ is assumed as a discrete-time function and is defined within a finite time interval (T_{ANBIT}), see **Figure 4** (optionally, APC can also be constructed from continuous-time anbits, see Conclusion and Section S6, Supporting Information).

Here, in line with the communication system shown in Figure 3, an encoder maps the user information onto the moduli and phases of $\psi_0 = |\psi_0|\, e^{i\angle_0}$ and $\psi_1 = |\psi_1|\, e^{i\angle_1}$, and a modulator converts the anbit amplitudes into optical waves utilizing two classical optical wave packets, e.g. with a rectangular temporal shape for simplicity (quasi-rectangular in practice), propagated in the fundamental modes of two parallel uncoupled waveguides, a technique termed **space-anbit modulation** (see Figure 4 and Methods). Note that ψ_0 and ψ_1 are defined in different time intervals T_0 and T_1 (with $T_0 = T_1$ or $T_0 \neq T_1$), and the time delay ΔT from ψ_0 to ψ_1 establishes a differential phase $\angle_1 - \angle_0 = 2\pi f_c \Delta T$, where f_c is the frequency of the optical carrier (since $\Delta T \sim 1/f_c$, then ΔT is within the scale of the optical cycle). Alternative physical implementations of an anbit can be proposed by exploring the mode, polarization, frequency, and time domains, giving rise to different anbit modulation formats (Section S1.1, Supporting Information). Moreover, the following noteworthy features of an anbit should be highlighted:

- *Vector space*. In the single-anbit vector space $\mathcal{E}_1 = \mathrm{span}\{\mathbf{e}_0, \mathbf{e}_1\}$, the standard complex inner product $\langle\cdot|\cdot\rangle$ allows us to define a norm $\|\boldsymbol{\psi}\| := \sqrt{\langle\boldsymbol{\psi}|\boldsymbol{\psi}\rangle} = \sqrt{|\psi_0|^2 + |\psi_1|^2}$ whose square provides information about the optical power ($\mathcal{P}$) propagated by the waveguides depicted in Figure 4a (see Methods).
- *Dimension*. Although, in general, we will work in a vector space with dimension $d = 2$, we have the possibility of defining the unit of information in a Hilbert space with $d \geq 1$, leading to different versions of APC termed d-APC (the usual case with $d = 2$ will be referred to as APC for short). In Supporting Section 4, we discuss how to construct the theory with $d \neq 2$.
- *Anbit measurement and degrees of freedom*. At the receiver, the demodulator recovers the anbit from the optical waves (which will be later processed by a decoder and a recipient source in the electrical domain, as commented in Section 2). Using terminology similar to that of quantum information,[10,44] the demodulation task will be referred to as the anbit measurement and can be carried out via two different ways in PIP: (*i*) a coherent measurement, implementable using coherent detection, or (*ii*) a differential measurement, associated to a direct detection scheme (Figure 4b). The former retrieves the moduli and phases of $\psi_{0,1}$ (4 real degrees of freedom) and the latter only provides information about $|\psi_{0,1}|^2$ and $\angle_1 - \angle_0$ (3 real degrees of freedom, the differential phase $\angle_1 - \angle_0$ is recovered from the time delay ΔT between the photocurrents, but the global phase of the anbit cannot be measured, see Section S1.2, Supporting Information). Hence, the number of **effective degrees of freedom** (EDFs) where the user information can be encoded at the transmitter depends on the kind of anbit measurement employed at the receiver. Thus, a given APC system will operate with anbits of 3 (or 4) EDFs when the receiver uses differential (or coherent) measurement. Although a differential measurement provides the lowest number of EDFs, it is the most economical strategy in a PIP platform.
- *Geometric representations*. An anbit with 4 EDFs can be geometrically represented by using a polar diagram illustrating the moduli and phases of $\psi_{0,1}$ (Figure 4c). An anbit with 3 EDFs may be represented in the **generalized Bloch sphere** (GBS), with a radius different from 1 (Figure 4d).

- *Multiple anbits*. A multi-anbit system will require to operate in a vector space "higher" than $\mathcal{E}_1$. The construction of such a vector space can be carried out by using the **tensor product** ($\otimes$)[51] or the **Cartesian product** ($\times$).[52] The former will allow us to extrapolate multi-anbit gates from quantum computing (e.g., controlled gates, see below). The latter will be of great benefit to construct multi-anbit linear operations that would otherwise exhibit a nonlinear nature using the tensor product (e.g., the fan-in and fan-out gates, see below). In Section S1.5, Supporting Information, we detail the main properties of the tensor and Cartesian products within the framework of APC.

Despite the fact that the anbit is similar to the qubit (and to its classical counterpart, the cebit,[32,33]) the following **fundamental differences** should be highlighted: (*1*) the anbit norm may be different from 1 and can be modified using a non-unitary operation, (*2*) the vector superposition of $\mathbb{e}_0$ and $\mathbb{e}_1$ is preserved after an anbit measurement, see Figure 4b (a feature also observed in a cebit measurement but not in a qubit measurement), (*3*) an anbit has 1 or 2 more EDFs than the qubit and the cebit (a direct consequence of (*1*) and (*2*)), (*4*) multiple anbits can be composed by using not only the tensor product but also the Cartesian product, (*5*) an anbit may be defined in a one-dimensional vector space (qubits and cebits cannot be restricted to one dimension given that a global phase is not observable in quantum waves[51] and in classical wave-optics based on direct detection[32]). However, in contrast to quantum computing, in APC we will not be able to perform instantaneous non-local operations (i.e., the entanglement of multiple anbits) because the underlying physical laws are deterministic,[53] a computational limitation that is also shared by any classical emulation of quantum computing.[32–40]

Furthermore, taking into account the vector formalism required to describe an anbit and its mathematical similitude with a qubit, let us introduce at this point the use of **Dirac's notation**[43,54,55] in order to: (*i*) simplify the mathematical calculations when designing complex APC computing architectures and (*ii*) extrapolate diverse analysis and design strategies from quantum computing, preserving the same notation between both computation theories. Therefore, from now on, let us express the anbit as $|\psi\rangle = \psi_0\ |0\rangle + \psi_1|1\rangle$, with $\boldsymbol{\psi} \equiv |\psi\rangle$, $\mathbb{e}_0 \equiv |0\rangle$, and $\mathbb{e}_1 \equiv |1\rangle$.

4. Basic Anbit Operations

The second natural step to construct a computation theory is to introduce the basic computational operations: the **anbit gates**. Since PIP is a hardware platform capable of integrating non-feedback and feedback circuits,[12–16] APC operations should be respectively classified in **two principal classes** (Figure 2): combinational and sequential. In a **combinational** operation, the output anbits depend solely on the input anbits. Contrariwise, in a **sequential** operation, the output anbits can be connected with the input anbits allowing feedback systems. In this section, we will first describe the basic combinational anbit gates and, second, we will present the fundamental concepts to design sequential anbit operations. In both scenarios, we will detail their technological implementations by using PIP circuitry.

4.1. Fundamentals of Combinational Design

Given that APC systems should be readily implementable with PIP technology, it is natural to ask how the mainstream PIP devices (phase shifters, beam splitters, beam combiners, attenuators, amplifiers, and resonators) may be employed to transform anbits. The answer depends on our ability to define basic anbit gates that mirror the wave transformations performed by these devices. To this end, we should first introduce the basic anbit operations in abstract terms, and later we will specify their PIP implementation.

The simplest anbit operation that can be built is a gate of a single anbit: a combinational (i.e., **non-feedback**) system carrying out a transformation between two different anbits, the input anbit $|\psi\rangle = \psi_0\ |0\rangle + \psi_1|1\rangle$ and the output anbit $|\varphi\rangle = \varphi_0\ |0\rangle + \varphi_1|1\rangle$ (**Figure 5**a). Mathematically, the gate is described via an arbitrary mapping (or operator) $\mathbb{F} : \mathcal{E}_1 \rightarrow \mathcal{E}_1$, which will be assumed to be a holomorphic function for convenience. In this way, such a mapping can be written as a power series $\mathbb{F} = \mathbb{F}^{(1)} + \mathbb{F}^{(2)} + \mathbb{F}^{(3)} + \cdots$, with $\mathbb{F}^{(k)}$ accounting for the linear ($k = 1$) and nonlinear ($k > 1$) responses of the gate. Considering that PIP circuits typically implement linear wave transformations via matrix signal processing,[13] we will focus our attention on the case $\mathbb{F} \equiv \mathbb{F}^{(1)}$: **linear gates** constructed from **matrix algebra** (see below). Nonetheless, it is worth mentioning that we will also be able to implement nonlinear anbit gates with PIP technology (constructed from tensor algebra, see Methods), extending the applicability of APC to solve computational problems requiring both linear and nonlinear operations (see Section 5).

Specifically, a single-anbit linear gate is a linear operator $\mathbb{F}$ exhibiting the following general properties:

- *Uniqueness*. The input and output anbits are always related by a unique linear operator $\mathbb{F}$. This property directly follows from the uniqueness of a linear transformation between vector spaces.[56]
- *Matrix representation*. Given an orthonormal vector basis $\mathcal{B}_1 = \{|0\rangle, |1\rangle\}$, the matrix representation of $\mathbb{F}$ is unique and is given by the expression:

$$F = \begin{bmatrix} \langle 0|\mathbb{F}|0\rangle & \langle 0|\mathbb{F}|1\rangle \\ \langle 1|\mathbb{F}|0\rangle & \langle 1|\mathbb{F}|1\rangle \end{bmatrix} \tag{1}$$

Hence, the gate can equivalently be described by the matrix F and the input-output relation $|\varphi\rangle = \mathbb{F}\ |\psi\rangle$ can be expressed as the vector-by-matrix multiplication $[|\varphi\rangle]_{\mathcal{B}_1} = F[|\psi\rangle]_{\mathcal{B}_1}$, where $[|\varphi\rangle]_{\mathcal{B}_1} = (\varphi_0\ \varphi_1)^T$, $[|\psi\rangle]_{\mathcal{B}_1} = (\psi_0\ \psi_1)^T$, and T denotes the transpose matrix (see Sections 1.4 and 2.1, Supporting Information).

- *Reversibility*. By definition, a gate is reversible when $\mathbb{F}$ is a bijective mapping. In such circumstances, $\det(F) \neq 0$ and the input anbit can be recovered from the output anbit by applying the inverse mapping $\mathbb{F}^{-1}$, whose matrix representation is F^{-1}. In contrast, a gate is irreversible when $\det(F) = 0$ and the input anbit cannot be retrieved from the output anbit given that $\mathbb{F}^{-1}$ does not exist.
- *Non-locality*. The input-output relation $|\varphi\rangle = \mathbb{F}\ |\psi\rangle$ is non-local and causal. The input and output anbits are respectively

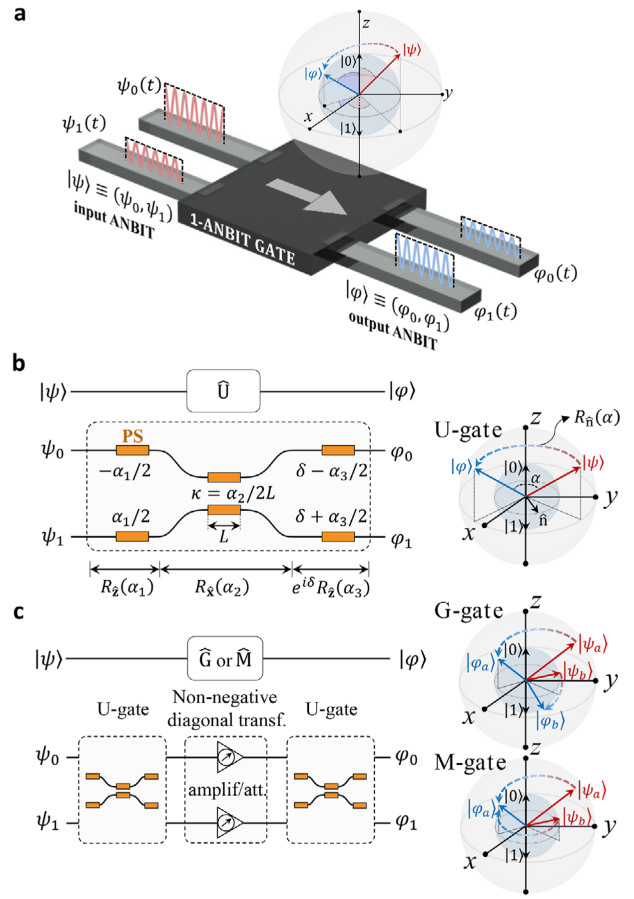

Figure 5. Basic combinational single-anbit linear gates. a) A combinational single-anbit gate is a non-feedback system performing a transformation between two different 2D vectors: the input anbit $|\psi\rangle = \psi_0|0\rangle + \psi_1|1\rangle$ and the output anbit $|\varphi\rangle = \varphi_0\,|0\rangle + \varphi_1|1\rangle$. If such a transformation is linear and we use anbits with 3 EDFs, the gate can be geometrically represented as a trajectory between two different points located on the same GBS (U-gate) or different GBSs with dissimilar radii (G- and M-gates). b) Minimal circuit architecture (MCA) of a U-gate, implementing the universal unitary matrix of Equation (2) via the Euler factorization $U = e^{i\delta}\ R_{\hat{n}}(\alpha) \equiv e^{i\delta} R_{\hat{z}}(\alpha_3) R_{\hat{x}}(\alpha_2) R_{\hat{z}}(\alpha_1)$.[31] The U-gate generates a rotation around an arbitrary unit vector $\hat{n}$ of the GBS, preserving the norm of the input anbit. c) MCA of a G- and M-gate, based on the singular value decomposition. While a G-gate is a reversible operation (two different input anbits $|\psi\rangle_a$ and $|\psi\rangle_b$ are always transformed into two different output anbits $|\varphi\rangle_a$ and $|\varphi\rangle_b$), an M-gate may be an irreversible operation (two different input anbits $|\psi\rangle_a$ and $|\psi\rangle_b$ may generate the same output anbit $|\varphi\rangle_a$). (PS: phase shifter).

implemented by two different electric fields $\mathbf{E}(\mathbf{r}_1, t_1)$ and $\mathbf{E}(\mathbf{r}_2, t_2)$ with $\mathbf{r}_1 \neq \mathbf{r}_2$ and $t_1 < t_2$ (see Methods).

- *Classes of linear gates.* Since PIP technology is able to implement optical systems whose transfer matrices may be unitary or non-unitary,[13] we define the following classes of linear anbit operations based on matrix algebra:[57] unitary gates (**U-gates**), general linear gates (**G-gates**) and general matrix gates (**M-gates**). Concretely, the U-gates will account for the linear reversible mappings that preserve the norm of the input anbit (conservative operations) via a unitary matrix transformation (Figure 5b). Contrariwise, the G- and M-gates will describe non-conservative linear operations (Figure 5c). While, by definition, a G-gate is always reversible, an M-gate may be reversible or irreversible, encompassing both possibilities. Hence, a G-gate will be described by a general linear (i.e., non-singular) matrix, whereas an M-gate will be associated to a general complex matrix (singular or non-singular).
- *Geometric representation.* Using differential measurement (which will be the case in most PIP platforms), a single-anbit gate may be geometrically interpreted as a trajectory between two points located on the same GBS (U-gate) or different GBSs with dissimilar radii (G- and M-gates), see Figure 5. Specifically, the kind of trajectory depends on the class of the gate, see Section S2.1, Supporting Information for more details.
- *Universal matrices.* The U- and G-gates belong to the U(2) and GL(2, ℂ) Lie groups, respectively, while an M-gate belongs to the $\mathfrak{gl}(2,\mathbb{C})$ Lie algebra.[57] Using the fundamentals of these algebraic structures,[10,31,57,58] it is straightforward to find a universal (or arbitrary) matrix in each class of gate, which must be able to describe all the possible 2×2 matrix transformations associated to the class when varying the value of its entries, encoded by parameters. In particular, a universal matrix of a U-gate reads as follows:[10,31]

$$U = e^{i\delta} R_{\mathbf{n}}(\alpha) = e^{i\delta} \begin{pmatrix} \cos\frac{\alpha}{2} - in_z \sin\frac{\alpha}{2} & -\left(n_y + in_x\right)\sin\frac{\alpha}{2} \\ \left(n_y - in_x\right)\sin\frac{\alpha}{2} & \cos\frac{\alpha}{2} + in_z\sin\frac{\alpha}{2} \end{pmatrix} \quad (2)$$

where $\delta \in [0, 2\pi)$ is a global phase shifting and $R_{\mathbf{n}}(\alpha)$ is a rotation matrix accounting for a rotation of an angle $\alpha \in [0, 2\pi]$ around an arbitrary unit vector $\mathbf{n} = n_x\,\mathbf{x} + n_y\mathbf{y} + n_z\mathbf{z}$ in the GBS (Figure 5b). Note that Equation (2) is constructed by using 4 independent real parameters (δ, α and two components of $\mathbf{n}$), according to the dimension of U(2).[31,58] On the other hand, a possible universal matrix of a G- or M-gate is a parametric matrix (denoted as G or M, respectively) with the four entries described by four independent complex numbers (8 independent real parameters, in line with the dimension of GL(2, ℂ) and $\mathfrak{gl}(2,\mathbb{C})$).[57,58] Nevertheless, in the former case (G-gate), the condition $\det(G) \neq 0$ must be fulfilled.

- *PIP implementation.* The optical implementation (or circuit architecture) of a U-, G-, or M-gate must be able to perform the 2×2 matrix transformation described by its universal matrix by utilizing basic PIP devices. Since a universal matrix may be implementable by different equivalent circuit architectures, we should introduce here the concept of **minimal circuit architecture** (MCA), defined as the PIP implementation encompassing the minimum number of basic devices. Furthermore, since any PIP circuit is fully characterized by analyzing the Lorentz reciprocity and the forward-backward (FB) symmetry (basic physical properties of an optical system that are not equivalent,[13]) we include an extended discussion about these properties within the context of APC in Section S2.1, Supporting Information.

Uncovering the MCA of the U-, G-, and M-gates requires to explore diverse matrix factorization techniques that allow us to implement the universal matrix of each class of operation by utilizing PIP technology. After a thorough examination of the matrix theory literature,[10,52,56–62] two different factorization techniques should be taken into consideration in our discussions: Euler's rotation theorem and the singular value decomposition.

As reported in ref.,[31] a 2×2 universal unitary matrix of the form given by Equation (2) cannot be directly implemented by using mainstream PIP devices because of the arbitrary nature of $\mathbf{n}$. Here, we can take advantage of Euler's rotation theorem to factorize the U matrix as a concatenation of three rotations around two Cartesian axes of the GBS, which are implementable via phase shifters, directional couplers, and multimode interferometers. In addition, taking into account that a U-gate can be regarded as a 2×2 universal unitary signal processor, then the MCA of a U-gate (Figure 5b) must be the same as the MCA of a 2 × 2 universal unitary signal PIP processor, shown in Figure 4a of ref.[31] and based on the Euler factorization $U = e^{i\delta} R_{\mathbf{n}}(\alpha) \equiv e^{i\delta} R_{\mathbf{z}}(\alpha_3) R_{\mathbf{x}}(\alpha_2) R_{\mathbf{z}}(\alpha_1)$. The matrices $R_{\mathbf{z}}(\alpha_{1,3})$ can be implemented by phase shifters integrated in parallel uncoupled waveguides and the matrix $R_{\mathbf{x}}(\alpha_2)$ may be generated by a synchronous directional coupler with tunable mode-coupling coefficient $\kappa = \alpha_2 /(2L)$, where L is the length of its arms. This MCA preserves the Lorentz reciprocity but breaks the FB symmetry (provided that $\alpha_1 \neq \alpha_3$). Equivalent circuit architectures of a U-gate may be explored by selecting different rotation vectors when using Euler's rotation theorem. As an example, Section 2.2, Supporting Information it is shown a scheme built from fixed couplers, based on the factorization $U = e^{i\delta} R_{\mathbf{z}}(\alpha_3) R_{\mathbf{y}}(\alpha_2) R_{\mathbf{z}}(\alpha_1)$.

While a U-gate is a conservative transformation (given that it preserves the norm of the input anbit or, equivalently, the power of the 2D wave that implements the anbit), both G- and M-gates are non-conservative transformations. This implies that their MCAs will require to include attenuators and amplifiers. Remarkably, a common MCA for both kind of gates is found from the singular value decomposition,[52,56,59] which factorizes the universal matrices of these gates as a function of two U-gates along with a 2 × 2 diagonal matrix with positive real entries, implementable by using tunable optical attenuators and amplifiers (Figure 5c). The reciprocal (non-reciprocal) nature of such devices preserves (breaks) the Lorentz reciprocity in the MCA. Likewise, note that the FB symmetry is broken in the MCA when using the circuit of Figure 5b to implement the U-gates.

Although equivalent circuit architectures of the U-, G-, and M-gates can be proposed by using matrix factorizations different from Euler's rotation theorem and the singular value decomposition, all of them lead to optical schemes integrating a higher number of basic PIP devices than the structures depicted in Figure 5 (see Section S2.2, Supporting Information).

So far, we have presented the basic single-anbit operations. Nonetheless, keeping in mind that PIP is a hardware that is reconfigurable via control signals,[12–14] the design of complex combinational architectures will be simplified by introducing an additional fundamental piece in APC: a **controlled gate**. Such a kind of operation is usually present in any computation theory,[10,43], e.g., in quantum computing, where a controlled gate is indispensable: (*i*) to enable or disable a computational operation on the qubits and (*ii*) to scale the quantum computing systems.[10] Therefore, taking into account the mathematical similarities between quantum computing and APC, we will define a controlled gate in APC in the same way as in quantum computing.[10] By convention, a controlled anbit gate performs a transformation $\mathbb{F}$ on the target anbits when the control anbits are equal to $|1\rangle$. Otherwise, the target anbits remain invariant at the output. **Figure 6**a illustrates the functionality of a controlled gate with a single **target anbit** $|t\rangle$ and a single **control anbit** $|c\rangle$. Using the tensor product, the mathematical formalization and properties of a controlled gate in APC can be directly extrapolated from quantum computing (Section S2.3, Supporting Information), with the significant difference that a controlled gate may be constructed from a non-unitary $\mathbb{F}$ transformation in APC.

An additional crucial difference between APC and quantum computing in a controlled gate emerges when analyzing its implementation using PIP technology. Since the reconfigurability of a PIP circuit is realized by utilizing classical electrical control signals,[12–14] the implementation of a controlled anbit gate does not require the intricate design strategies and architectures employed in optical quantum computation[10,29,63,64] (however, these schemes could be extrapolated to APC, if desired). As seen in Figure 6b, the simplest implementation of a controlled anbit gate arises from an electro-optic design, where the control anbit is mapped onto the electrical control signals of the PIP platform and the target anbit is implemented with a 2D optical wave (alternatively, both control and target anbits can be implemented with optical waves, giving rise to an all-optical architecture requiring a higher footprint than that of the electro-optic design, see Figure 6c). In this fashion, the same MCAs as those of the U-, G-, and M-gates (Figure 5) may be employed to perform controlled operations of each kind of gate. Thus, the electro-optic architecture only entails the definition of a mapping between the states $|0\rangle$ and $|1\rangle$ of the control anbit and the electrical control signals of the PIP circuit, which can be directly established via software. Here, a non-ideal behavior of the hardware components (e.g., due to noise or manufacturing imperfections) could deviate the electrical control signals (implementing the state of the control anbit) from the ideal values, which could generate phase-shifter deviations and, consequently, additive noise onto the amplitudes of the target anbit. Nonetheless, it should be noted that this problem is not exclusive of a controlled anbit gate. In general, this problem can be found in any PIP platform implementing matrix transformations onto the optical signals,[13] where these phase-shifter deviations are mitigated by specific hardware-error-correction algorithms.[65–67]

As an illustrative example, the electro-optic implementation of the **controlled-NOT (CNOT) gate** is sketched in Figure 6d. Any suitable mapping between the control anbit and the electrical control signals must guarantee that the 2×2 unitary matrix transformations $F = \sigma_x = iR_{\mathbf{x}}(\pi)$ (a Pauli matrix) and $F = I$ (the identity matrix) are induced on the amplitudes of $|t\rangle$ when $|c\rangle = |1\rangle$ and $|c\rangle = |0\rangle$, respectively. It is worthy noting that, in contrast to the seminal optical implementation of the quantum CNOT gate reported in ref.,[63] in APC the implementation of this gate integrates a reduced number of basic devices and does not require to use extra (ancilla or garbage) units of information.

Interestingly, the concept of controlled gates can be easily extended to the case of multiple control anbits without requiring extra devices in the PIP circuits, a feature of APC that cannot be found in optical quantum computation.[64] Accordingly, multi-controlled operations such as the **Toffoli gate** (an indispensable tool to implement Boolean functions) can be carried out in APC using the same circuit as that of Figure 6d by encoding an

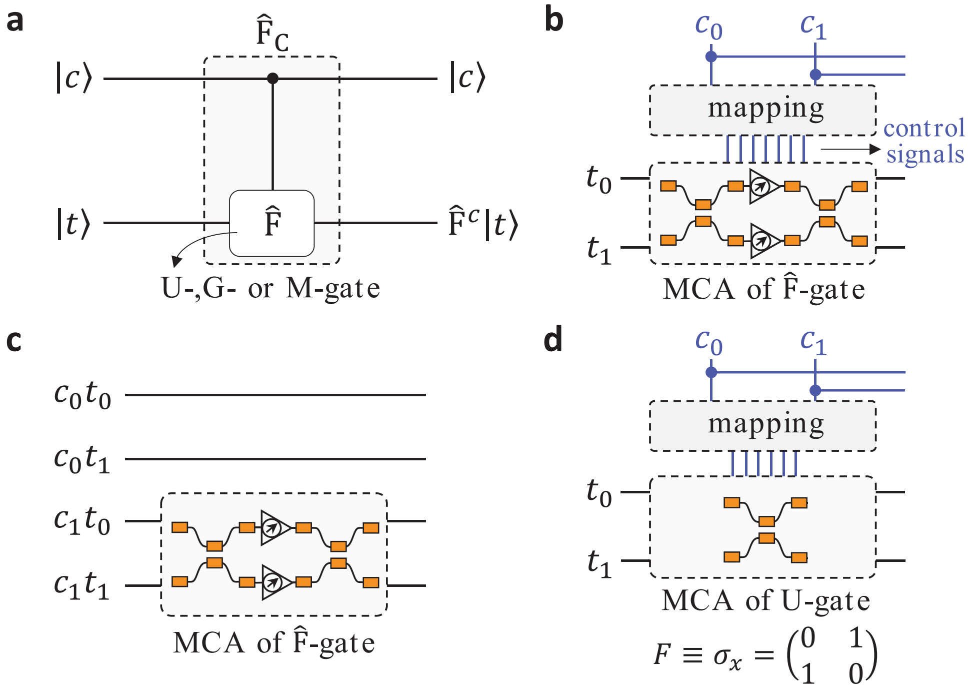

Figure 6. Controlled anbit gates. a) Symbolic representation and functionality of a controlled gate $\mathbb{F}_C$ with a single control anbit $|c\rangle \in \{|0\rangle, |1\rangle\}$ and a single target anbit $|t\rangle$. Inspired in a controlled quantum gate, the operation $\mathbb{F}$ (associated to a U-, G-, or M-gate) is applied to $|t\rangle$ when $|c\rangle = |1\rangle$ or, otherwise, $|t\rangle$ remains invariant at the output. b) Electro-optic design of the controlled gate $\mathbb{F}_C$. The PIP circuit must implement the MCA of the $\mathbb{F}$-gate (here we depict the MCA of an M-gate to cover the general case), whose basic optical devices are controlled by electrical signals (blue lines) mapped with the amplitudes of $|c\rangle = c_0\,|0\rangle + c_1|1\rangle$ via software.[66] The optical inputs encode the amplitudes of $|t\rangle = t_0\,|0\rangle + t_1|1\rangle$ (black lines). c) All-optical design of the controlled gate $\mathbb{F}_C$. The optical inputs encode the amplitudes of $|c\rangle \otimes |t\rangle$, where $\otimes$ is the tensor product. d) Electro-optic implementation of the controlled-NOT anbit gate. The PIP circuit is the MCA of a U-gate since $F = \sigma_x$ is a unitary matrix.

additional control anbit in the electrical control signals, see Section S2.3, Supporting Information.

4.2. Fundamentals of Sequential Design

From a signal processing perspective, feedback systems are crucial configurations in a PIP platform to implement applications out of the scope of non-feedback schemes, e.g., filters with infinite impulse response.[13] Therefore, from a computational perspective, we wonder about the potential applications of feedback PIP circuits within the context of APC. To this end, we introduce the concept of sequential anbit operations where, in contrast to a combinational gate, the output anbits can be connected with the input anbits leading to **feedback** computational architectures (**Figure 7**).

Remarkably, in contrast to quantum computation, feedback schemes will be allowed in APC thanks to the feasibility of performing summation (**fan-in**) and cloning (**fan-out**) of anbits using PIP circuits. These are prohibited operations within the realm of quantum computing that will however play a fundamental role to construct any sequential architecture in APC. Concretely, both fan-in and fan-out anbit gates can be implemented via the PIP circuit depicted in Figure 7a, which preserves the Lorentz reciprocity and the FB symmetry (provided that the amplifiers have a reciprocal and FB symmetric behavior). This scheme transforms the input anbits $|\psi\rangle$ and $|\varphi\rangle$ into the output anbits $|\psi + \varphi\rangle = (\psi_0 + \varphi_0)\,|0\rangle + (\psi_1 + \varphi_1)|1\rangle$ and $|\psi - \varphi\rangle = (\psi_0 - \varphi_0)\,|0\rangle + (\psi_1 - \varphi_1)|1\rangle$. Thus, setting $|\varphi\rangle = |0\rangle = 0|0\rangle + 0|1\rangle$ (the null vector of $\mathcal{E}_1$) we will carry out a fan-out operation on the anbit $|\psi\rangle$ (a perfect cloning) and taking $|\varphi\rangle \neq |0\rangle$ we will perform a fan-in operation on the anbits $|\psi\rangle$ and $|\varphi\rangle$. Moreover, in order to guarantee a linear behavior, both fan-in and fan-out gates should be defined by using the Cartesian product, which allows us to independently transform the anbit amplitudes ψ_0, ψ_1, φ_0 and φ_1 (conversely, the tensor product leads to multi-anbit nonlinear operations, see Supporting Section 3.1, Supporting Information, including a more in-depth discussion about the mathematical properties and optical implementation of these gates).

Figure 7b shows the simplest sequential architecture that can be built in APC, integrated by both fan-in and fan-out gates along with two M-gates ($\mathbb{M}_1$ and $\mathbb{M}_2$) to complete the feedback loop. The analysis of the input-output relation $|\varphi\rangle = \mathbb{M}_{eq}\,|\psi\rangle$ indicates that this sequential scheme is equivalent to a combinational M-gate described by the matrix $M_{eq} = (I - M_1M_2)^{-1}\,M_1$. Hence, the existence of M_{eq} is closely linked to the condition $\det(I - M_1M_2) \neq 0$. Contrariwise, the loop cannot be built because the matrix $I - M_1M_2$ is singular. In Section S3.2, Supporting Information, we provide further information about the analysis and properties of this structure. Although the same single-anbit operation $\mathbb{M}_{eq}$ can be implemented via the MCA of an M-gate (Figure 5c), the potential of this basic sequential scheme relies on the fact that it establishes the fundamental strategies to analyze and design more complex sequential architectures in APC,

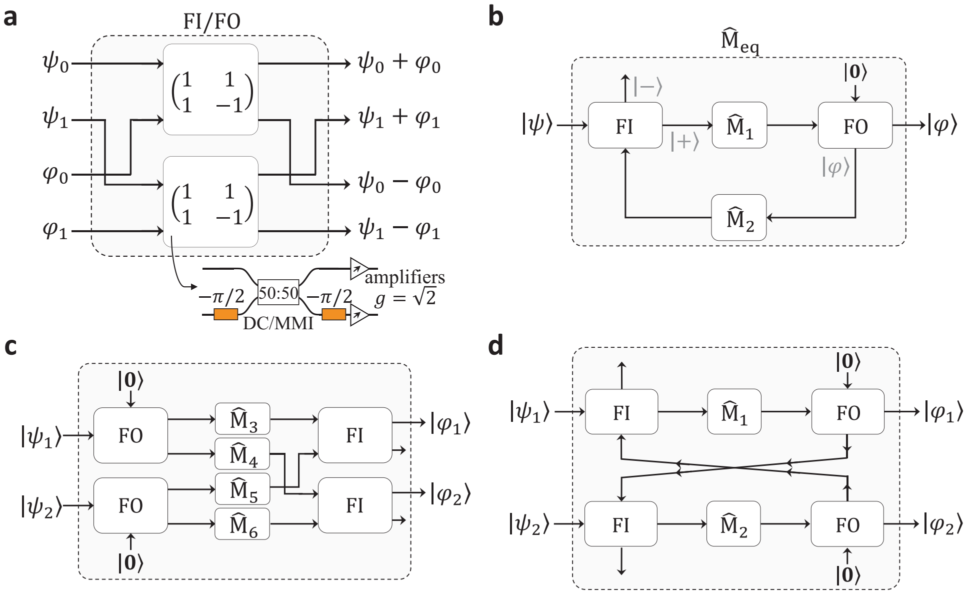

Figure 7. Sequential anbit systems. a) Optical implementation using PIP technology of both fan-in (FI) and fan-out (FO) anbit gates. The FI operation maps the input $|\psi\rangle \times |\varphi\rangle$ into the output $|\psi\rangle + \varphi \times |\psi\rangle - \varphi$, where $\times$ is the Cartesian product. The FO operation performs a perfect cloning of $|\psi\rangle$ when $\varphi_0 = \varphi_1 = 0$, i.e., taking $|\varphi\rangle = |\mathbf{0}\rangle$, where $|\mathbf{0}\rangle = 0|0\rangle + 0|1\rangle$ is the null anbit. b) Sequential system of a single anbit, composed by both FI and FO gates along with 2 single-anbit M-gates ($\mathbb{M}_1$ and $\mathbb{M}_2$). c) Multi-anbit combinational system composed by 4 single-anbit M-gates, 2 FI gates, and 2 FO gates. d) Equivalent multi-anbit sequential system, integrating 2 single-anbit M-gates, 2 FI gates, and 2 FO gates. (DC: directional coupler. MMI: multi-mode interferometer).

which will allow us to uncover unexpected applications of such a kind of systems.

For instance, the intricate multi-anbit combinational scheme shown in Figure 7c can be replaced by the sequential architecture depicted in Figure 7d, composed by a lower number of gates. Surprisingly, using the Cartesian product, we find that both systems are governed by an input-output relation of the form:

$$|\varphi_1\rangle \times |\varphi_2\rangle = \mathbb{F}_1 \, |\psi_1\rangle \times |\psi_1\rangle + \mathbb{F}_2 \, |\psi_2\rangle \times |\psi_2\rangle \tag{3}$$

Here, taking $\mathbb{F}_1 \equiv \mathbb{M}_3 \times \mathbb{M}_4$ and $\mathbb{F}_2 \equiv \mathbb{M}_5 \times \mathbb{M}_6$, we recover the input-output relation of the circuit sketched in Figure 7c, and setting $\mathbb{F}_1 \equiv [(1 - \mathbb{M}_1\mathbb{M}_2)^{-1}\mathbb{M}_1] \times [(1 - \mathbb{M}_2\mathbb{M}_1)^{-1}\mathbb{M}_2\mathbb{M}_1]$ and $\mathbb{F}_2 \equiv [(1 - \mathbb{M}_1\mathbb{M}_2)^{-1}\mathbb{M}_1\mathbb{M}_2] \times [(1 - \mathbb{M}_2\mathbb{M}_1)^{-1}\mathbb{M}_2]$, we obtain the input-output relation of the circuit shown in Figure 7d (see Section S3.3, Supporting Information). Consequently, both computational schemes are found to be equivalent, provided that the $\mathbb{M}_1$ and $\mathbb{M}_2$ gates of the sequential system lead to the same $\mathbb{F}_{1,2}$ operators in Equation (3) as those of the multi-anbit combinational architecture. This result unveils a potential application of sequential gates: the simplification of multi-anbit combinational systems, which paves the way for the **scalability** of APC structures.

A possible technological difficulty might arise when integrating optical amplifiers within a feedback loop, which may give rise to undesirable nonlinear and lasing effects. This is a well-known implementation problem in PIP when designing feedback architectures (e.g., in photonic waveguide meshes) that is circumvented by normalizing the transfer matrices of the PIP systems (whose circuitry only requires passive devices) and carrying out the amplification stages outside of the meshes by external dedicated high-performance blocks.[12] Furthermore, these dedicated blocks prevent the propagation of amplified spontaneous emission noise inside the meshes and, at the same time, preserve the FB symmetry of the tunable basic units. Fabrication techniques such as micro-transfer printing enable the integration of amplifiers in silicon PIP platforms, allowing arbitrary placement of III-V semiconductor materials compatible to silicon features.[68,69]

5. Computational Problems and Roadmap

Once the basic operations of APC have been introduced, the next natural step is to discuss the type of mathematical problems that may be computed. As detailed in Section 4 (Methods), linear (nonlinear) anbit operations are described by matrices (tensors). Consequently, the problems that can be solved by APC correspond to those that are computable by an algorithm based on linear and nonlinear operations that can be expressed with **matrix and tensor** algebra, respectively.

There are numerous applications in mathematics, physics, and (bio) engineering that can be efficiently solved by utilizing matrix algorithms, such as artificial intelligence,[70] deep learning,[71] tensor decomposition,[72] astronomical imaging,[73] robotics,[74] drug design,[75,76] autonomous driving,[77] medical diagnostic imaging,[78] and genomic analysis.[79,80] Most of these applications involve **pattern recognition**, a computational task that can be conducted with quantum computers, e.g., using the single-qubit model reported in refs.[81, 82] Remarkably, this computing method may be directly extrapolated to APC by using single-anbit U-gates (Figure 5b). Alternatively, pattern recognition can also be tackled with single-anbit gates by mimicking the one-neuron model recently proposed in ref.[83] This exclusively requires to use M-gates (Figure 5c) and nonlinear single-anbit operations to carry out the feedback loops and the activation function of the neuron, respectively.

In addition, a range of mathematical and physical problems can be computed with single-anbit operations. As is well known, any system of linear equations can be written in matrix form as $A \cdot \mathbf{x} = \mathbf{b}$.[84] The solution of the system (if exists) is found from the vector-by-matrix multiplication $\mathbf{x} = A^{-1} \cdot \mathbf{b}$. In the 2D case, this operation may be conducted in APC with a single-anbit G-gate by identifying $\mathbf{b}$ as the input anbit, A^{-1} as the matrix of the G-gate (Figure 5c), and $\mathbf{x}$ as the output anbit. Likewise, APC will be able to handle any physical system governed by **differential or integral equations** that can be discretized in a matrix form by an algorithm.[85–87] The underlying idea of these algorithms is to transform the original differential or integral equation into iterative systems of linear equations of the form $A \cdot \mathbf{x} = \mathbf{b}$, which are computable by single-anbit G-gates in the 2D case, as commented above. Some illustrative examples are the Fredholm integral equation,[85] the heat equation,[86] and the Helmholtz equation.[87] In this way, a large variety of 2D quantum, photonic, acoustic, electric, and thermodynamic systems may be numerically analyzed and designed with the single-anbit operations and the PIP circuits shown in Figure 5.

Nonetheless, the resolution of large-scale computational problems based on matrix and tensor algorithms[72,88] will require to use multi-anbit operations, which should be developed in future research. In this vein, bearing in mind that this work is completely devoted to establishing the fundamentals of APC, a **roadmap** must be specified to complete this computation theory in forthcoming contributions.

Firstly, the fundamentals of combinational design should be extended to the case of multiple anbits for both U-, G-, and M-gates. We may expect that the MCA of these multi-anbit gates can also be employed to implement controlled gates with multiple target anbits (mapping the control anbits onto the electrical control signals of the PIP platform). Secondly, the fundamentals of sequential design should be further developed to the case of multiple anbits, embracing the research of fan-in, fan-out, and feedback operations. Given that a digital memory is built from a multi-bit sequential architecture in digital computing,[9] the study of multi-anbit feedback schemes could be of paramount importance to revisit the concept of memory within the scope of APC. Outstandingly, the capacity to scale both combinational and sequential architectures to multiple anbits is inherently related to the feasibility of scaling the PIP circuits by integrating multiple waveguides[12–14] in combination with the exploitation of wavelength-division multiplexing[27] to perform massive **parallel computing** of anbits. Here, it is also important to bear in mind the integration of external dedicated high-performance blocks when designing multi-anbit combinational and sequential architectures requiring amplification stages to preclude the generation of nonlinear and lasing effects, as well as the propagation of amplified spontaneous emission noise inside the PIP platform. Thirdly, a gamut of **specific search algorithms** based on anbit operations should be conceived to efficiently solve large-scale matrix and tensor computational problems.[72,88] The time, resources, and energy required in APC to solve these problems must be compared with the time, resources, and energy required in digital, quantum, and neuromorphic computing using the general methodologies of computational science.[10,89]

6. Conclusion

These results lay the theoretical foundations of APC, a new computing paradigm conceived to exploit the full potential of PIP technology and, consequently, leading to the emergence of an entire field of research within computational science and photonics. In addition, APC can be regarded as a new optical design toolbox that blazes a trail for manufacturing advanced photonic computing architectures that can team-up with digital electronic processors to unlock in the near- and middle-term the serious limitations imposed by the demise of Moore's and Dennard's laws.

Compared with these existing computational models, APC relaxes some of their theoretical and technological limitations, see **Table 1**. While in APC we have the possibility of defining both linear and nonlinear gates, digital and quantum computing are only constructed from nonlinear and linear gates, respectively.[9,10] Moreover, neuromorphic computing embraces both linear and nonlinear operations, but the global transformation induced on the units of information in a neural network is nonlinear.[26] In contrast, in APC there exists the possibility of exclusively performing linear or nonlinear operations (or a combination of both). A similar remark applies to the reversible and irreversible nature of the operations. Both design possibilities can be found in APC via the U-, G-, and M-gates, a feature that is not usually shared by the other computation theories.

On the other hand, an essential difference between digital computing and APC relies on the fact that a combinational APC architecture can take advantage of both forward and backward propagations of light to compute the double of units of information. The capacity to exploit both propagation directions will depend on our ability to combine and interconnect the single-anbit U-, G, and M-gates when scaling the proposal to multi-anbit combinational operations in subsequent contributions. In such a scenario, the same (a different) multi-anbit transformation will be induced in each propagation direction when the circuit preserves (breaks) the FB symmetry. This property also applies to quantum and neuromorphic computing when implementing the corresponding computational architectures via PIP circuitry.[6,64]

The additional properties shown in Table 1 highlight common differences of APC, digital, and neuromorphic computing versus quantum computing. The most characteristic feature of quantum computing (not shared by the other computation theories) is the entanglement of qubits, allowing to perform instantaneous non-local operations, which provide two significant computational advantages over classical approaches. First, quantum non-locality alleviates the exponential increase in hardware resources when scaling quantum computing architectures.[33,40] Second, the computational time required to solve some academic examples of non-deterministic polynomial time problems could significantly be reduced with instantaneous non-local operations.[10,53] Hence, the absence of entanglement in APC might impact on the above points. In spite of the fact that the former limitation might not be completely circumvented when scaling APC, it could be slightly mitigated: (*i*) carrying out parallel computing of anbits by leveraging on the benefits of wavelength-division multiplexing and (*ii*) combining the space-anbit modulation (requiring two waveguides per anbit) along with other modulation formats (e.g., the frequency- and time-anbit modulations, requiring a single waveguide per anbit, see Section S1.1, Supporting Information). The

Table 1. Qualitative features of digital computation, quantum computation, neuromorphic computation, and analog programmable-photonic computation.

Properties	Digital Computing	Quantum Computing	Neuromorphic Computing	Analog Programmable-Photonic Computing
Linear computation	No[a)]	Yes	No	Yes
Nonlinear computation	Yes	No	Yes	Yes
Reversible operations[b)]	No	Yes	No	Yes
Irreversible operations	Yes	No	Yes	Yes
Forward-backward propagation	No	Yes	Yes	Yes
Parallel computing	Yes	Yes	Yes	Yes
Summation, cloning and feedback	Yes	No	Yes	Yes
Instantaneous non-locality	No	Yes	No	No
Scalability with current technology	Yes	No	Yes	Yes
Operation at room temperature	Yes	No	Yes	Yes
Tolerance to environmental noise	Yes	No	Yes	Yes

[a)] Although digital computing operations are nonlinear, this does not imply that digital computation is not able to solve linear problems. Indeed, digital computation is a universal computing model, as inferred from the Church-Turing thesis.[2,10] [b)] In digital computation, reversible operations can also be defined, but with inefficient schemes requiring ancilla and garbage bits.[43] In quantum computation, all operations are reversible (excluding the quantum measurement, which can be deemed as a non-reversible operation).[44] In neuromorphic computation, the multi-dimensional transformation of a neural network is usually an irreversible operation since the nonlinear activation functions are, in general, non-bijective mappings and a different number of neurons per layer is commonly used.[26] Nevertheless, reversible neural networks have also been proposed to reduce memory requirements in specific deep learning applications.[104,105]

second constraint might be mitigated in APC by dequantizing algorithms of quantum computing,[90] a promising methodology to deal with the development of algorithms based on anbit operations by exploiting the similarities between anbits and qubits.

Being APC a computation theory relying on classical waves, it can be readily implemented by current technology operating at room temperature. Indeed, it is worth mentioning that APC can be implemented not only in a PIP hardware, but also in any technological platform enabling matrix signal processing such as in metamaterials,[17,18] in free-space optics,[5] in electronics,[36,91,92] and in acoustics.[93] Likewise, we may expect that this new computing paradigm has more tolerance to environmental noise than quantum computation due to the absence of decoherence (the classical vector superposition of an anbit cannot be annihilated by environmental interactions).[94] This subsequently implies that we will require less extra units of information than in quantum computing to detect and correct the data errors, simplifying the scalability of APC architectures.

An additional intriguing feature of APC arises from the general nature of its mathematical framework, inherited from the versatile properties of the anbit, allowing to implement (at least partially) other existing computing paradigms using APC architectures (Section S5, Supporting Information).

In fact, the general nature of APC is also embodied in the possibility of conceiving the anbit as a continuous-time function. This gives rise to a different version of APC, termed **continuous-time APC**, which entails the use of **time-varying** optical media,[95] an attractive proposal to take advantage of future dynamical PIP systems, where the circuit transfer matrices could be modulated at the same time as the signals are propagated (e.g., by utilizing strongly-nonlinear epsilon-near-zero media[96] and phase change materials.[97,98]). Continuous-time APC handles computational problems with an approach inspired by adiabatic quantum computing:[99] the user information is mapped onto the temporal shape of $|\psi(t)\rangle$, which is transformed by a time-varying computational system within a finite time interval $t_1 \leq t \leq t_2$. The solution of the computational problem will be encoded by $|\psi(t > t_2)\rangle$. The potential of continuous-time APC relies on the possibility of solving differential and integral equations via dynamical vector-by-matrix multiplications, without requiring an iterative discretization of the equations. This could offer a simple route for the challenge of engineering the computational time of mathematical and physical problems based on differential and integral equations with varying coefficients. For completeness, in Section S6, Supporting Information, we sketch two computational examples of continuous-time APC.

Given that any computation theory is associated with an information theory, APC also leads to an additional field of research: the **Analog Programmable-Photonic Information**. Here, we will focus on the study of entropy, data compression (encoding the user information into the minimum number of anbits), modulation formats (converting the anbits into physical waves), channel capacity, analysis of noise, error detection, and correction strategies, and cryptography techniques. The combination of both computation and information theories has the potential to spark a crucial impact on fundamental and applied research, as well as on our information society.

7. Experimental Section

Space-Anbit Modulation: The description of this modulation format (similar to the path-encoding strategy employed in optical quantum computation[100]) can be done by specifying the electric field strength implementing the anbit of Figure 4a. According to the usual features of the optical waveguides employed in PIP,[13] we may assume that the parallel waveguides of Figure 4a have a negligible inter-waveguide mode-coupling and operate in the paraxial and single-mode regimes. Hence, a space-anbit modulation is characterized by an electric field of the form:

$$E(r,t) \simeq \sum_{k=0}^{1} \mathrm{Re}\left\{\psi_k\left(t-\beta_k^{(1)} r_{\parallel}\right)\hat{e}_k\left(r_{\perp,1}, r_{\perp,2}, \omega_c\right) e^{i\omega_c t} e^{-i\beta_k^{(0)} r_{\parallel}}\right\} = \sum_{k=0}^{1}\left|\psi_k\left(t-\beta_k^{(1)} r_{\parallel}\right)\right|\hat{e}_k\left(r_{\perp,1}, r_{\perp,2}, \omega_c\right)\cos\left(\omega_c t-\beta_k^{(0)} r_{\parallel}+\angle_k\right) \quad (4)$$

where the anbit amplitudes $\psi_0 = |\psi_0|\ e^{i\angle_0}$ and $\psi_1 = |\psi_1|\ e^{i\angle_1}$ play the role of the optical wave packets (or complex envelopes), ω_c is the angular frequency of the optical carrier, $r = r_{\perp,1}\hat{r}_{\perp,1} + r_{\perp,2}\hat{r}_{\perp,2} + r_{\parallel}\hat{r}_{\parallel}$ is the vector position written in terms of its transverse ($r_{\perp,1}$, $r_{\perp,2}$) and longitudinal ($r_{\parallel}$) components, and $\hat{e}_k$ and $\beta_k(\omega) \simeq \beta_k^{(0)} + (\omega-\omega_c)\beta_k^{(1)}$ are respectively the normalized mode profile and the propagation constant of the fundamental mode in waveguide k (being $\beta_k^{(0)} = \beta_k\ (\omega = \omega_c)$, $\beta_k^{(1)} = \mathrm{d}\beta_k(\omega = \omega_c)/\mathrm{d}\omega$, and omitting the dispersive terms $\beta_k^{(n\geq 2)}$ in the Taylor series expansion of $\beta_k(\omega)$). In particular, $\hat{e}_k$ must satisfy the condition:[101]

$$\iint_{-\infty}^{\infty} \hat{e}_k \times \hat{h}_k^{*} \cdot \hat{r}_{\parallel} \mathrm{d}r_{\perp,1} \mathrm{d}\, r_{\perp,2} = 2 \quad (5)$$

being $\hat{h}_k$ the normalized mode profile of the magnetic field strength. Equation (5) guarantees that the optical power ($\mathcal{P}$) propagated by the fundamental modes of both waveguides can be calculated as $\mathcal{P} = |\psi_0|^2 + |\psi_1|^2$.

Using Equation (4), it is straightforward to describe the electric field strength at the input $E(r_1, t_1)$ and at the output $E(r_2, t_2)$ of the single-anbit gate depicted in Figure 5a, which must be particularized at two different vector positions $r_1 \neq r_2$ and time instants $t_1 \neq t_2$. Taking into account the causal response of the materials employed in PIP,[13] then it follows that $t_1 < t_2$. Hence, the input-output relation of the gate is non-local and causal.

Nonlinear Anbit Gates: Nonlinear anbit operations could be implemented in PIP, e.g., by means of the Pockels and Kerr effects, which allow to carry out second- and third-order nonlinear anbit transformations, respectively. For instance, stimulating the self-phase modulation effect in two parallel uncoupled waveguides (similar to those of depicted in Figure 4a), a nonlinear single-anbit operation of the form $\mathbb{F}\ |\psi\rangle = \psi_0\ e^{-i\gamma|\psi_0|^2 L_{\mathrm{eff}}}|0\rangle + \psi_1 e^{-i\gamma|\psi_1|^2 L_{\mathrm{eff}}}|1\rangle$ may be obtained (γ and L_{eff} are nonlinear parameters of the waveguides.[102]). However, the capability of PIP is not only restricted to implementing second- and third-order nonlinear anbit transformations. In general, higher-order nonlinear operations can be performed in APC with PIP circuitry in the same vein as in neuromorphic computation arbitrary activation functions are generated by employing Mach–Zehnder interferometers and microring resonators.[103]

The most general definition of a single-anbit gate (including both linear and nonlinear contributions) is given by the expression $\mathbb{F}|\psi\rangle := f_0(\psi_0,\psi_1)|0\rangle + f_1(\psi_0,\psi_1)|1\rangle$, with f_0 and f_1 belonging to $\mathcal{F}(\mathbb{C}^2,\mathbb{C})$. Thus, $\mathbb{F}$ will induce a nonlinear transformation on the input anbit when the functions $f_{0,1}$ have a nonlinear behavior. Therefore, using holomorphic $f_{0,1}$ functions in a neighborhood of a reference point $(\psi_{0,\mathrm{ref}}, \psi_{1,\mathrm{ref}}) \in \mathbb{C}^2$, we will be able to build a nonlinear response of the desired order.

The main drawback of operating with nonlinear anbit gates relies on the fact that it could not deal with a matrix formalism. Nevertheless, the mathematical description of the above nonlinear anbit operation can be simplified by performing a Taylor series expansion of $f_{0,1}$. Therefore, let us introduce the vectors $z := \psi_0\hat{z}_0 + \psi_1\hat{z}_1$ and $z_{\mathrm{ref}} := \psi_{0,\mathrm{ref}}\hat{z}_0 + \psi_{1,\mathrm{ref}}\hat{z}_1$ belonging to the vector space $\mathcal{Z} = \mathrm{span}\{\hat{z}_0, \hat{z}_1\}$ (isomorphic to $\mathbb{C}^2$) and being $\hat{z}_{0,1}$ complex orthonormal vectors. In this way, we can write $\mathbb{F} = \sum_{n=1}^{\infty} \mathbb{F}^{(n)}$ where:

$$\hat{F}^{(n)}\ |\psi\rangle = \frac{1}{n!} d^n f_{0\mathbf{z}_{ref}}(\mathbf{z})\ |0\rangle + \frac{1}{n!} d^n f_{1\mathbf{z}_{ref}}(\mathbf{z})\ |1\rangle \quad (6)$$

is the n-th order nonlinear response of the gate with:

$$d^n f_{0\mathbf{z}_{ref}}(\mathbf{z}) = \sum\nolimits_{i_1,\ldots,i_n\in\{0,1\}} \psi_{i_1}\ldots\psi_{i_n} \frac{\partial^n f_0\left(\mathbf{z}_{ref}\right)}{\partial\hat{z}_{i1}\ldots\partial\hat{z}_{in}} \quad (7)$$

and similar for $\mathrm{d}^n f1\rfloor_{z\mathrm{ref}}(z)$. As seen, nonlinear anbit operations require a **tensor formalism** to describe the n-th order partial derivative of the above equation. This nonlinear mathematical framework should be further extended in forthcoming cssontributions by defining diverse classes of nonlinear anbit gates, encompassing both combinational and sequential computational architectures.

Supporting Information

Supporting Information is available from the Wiley Online Library or from the author.

Acknowledgements

This work was supported by the ERC-ADG-2022-101097092 ANBIT, ERC-POC-2023-101138302NUMESH, H2020-ICT-2019-021-871330 Neoteric, the Spanish MINECO Juan de la Cierva Incorporación program, Spanish MICIN Planes Complementarios Comunicacion Cuantica projects QUANTUMABLE-1 and 2, the Generalitat Valenciana PROMETEO 2017/017 research excellency award, and Infraestructuras FEDER IDIFEDER/2018/031, FEDER IDIFEDER/2020/032, and FEDER IDIFEDER/2021/050.

Conflict of Interest

The authors declare no conflict of interest.

Data Availability Statement

The data that support the findings of this study are available from the corresponding author upon reasonable request.

Keywords

information processing, integrated optics, optical computing, programmable integrated photonics

Received: May 18, 2022
Revised: July 6, 2023
Published online:

[1] R. K. Cavin, P. Lugli, V. V. Zhirnov, *Proc. IEEE Special Centenn. Issue* **2012**, *100*, 1720.
[2] I. L. Markov, *Nature* **2014**, *512*, 147.
[3] J. Shalf, *Philos Trans A Math Phys Eng Sci* **2020**, *378*, 20190061.

[4] T. Ferreira de Lima, B. J. Shastri, A. N. Tait, M. A. Nahmias, P. R. Prucnal, *Nanophotonics* **2017**, *6*, 577.
[5] G. Wetzstein, A. Ozcan, S. Gigan, S. Fan, D. Englund, M. Soljačić, C. Denz, D. A. B. Miller, D. Psaltis, *Nature* **2020**, *588*, 39.
[6] B. J. Shastri, A. N. Tait, T. F. de Lima, W. H. P. Pernice, H. Bhaskaran, C. D. Wright, P. R. Prucnal, *Nat. Photonics* **2021**, *15*, 102.
[7] B. J. Shastri, A. N. Tait, T. Ferreira de Lima, M. A. Nahmias, H. T. Peng, P. R. Prucnal, In *Encyclopedia of Complexity and Systems Science* (Ed.: R. Meyers), Springer, Berlin **2018**.
[8] T. C. Bartee, *Digital Computer Fundamentals*, McGraw-Hill, New York, **1985**.
[9] J. F. Wakerly, *Digital Design: Principles and Practices*, Pearson, New Jersey **2006**.
[10] M. A. Nielsen, I. L. Chuang, *Quantum Computation and Quantum Information*, Cambridge University Press, Cambridge, **2016**.
[11] D. R. Solli, B. Jalali, *Nat. Photonics* **2015**, *9*, 704.
[12] W. Bogaerts, D. Pérez, J. Capmany, D. A. B. Miller, J. Poon, D. Englund, F. Morichetti, A. Melloni, *Nature* **2020**, *586*, 207.
[13] J. Capmany, D. Pérez, *Programmable Integrated Photonics*, Oxford University Press, Oxford **2020**.
[14] D. Pérez, I. Gasulla, P. DasMahapatra, J. Capmany, *Adv. Opt. Photonics* **2020**, *12*, 709.
[15] L. Lu, L. Shen, W. Gao, L. Zhou, J. Chen, *IEEE Photonics J.* **2019**, *11*, 6603312.
[16] T. Sato, A. Enokihara, *Opt. Express* **2019**, *27*, 33005.
[17] M. Camacho, B. Edwards, N. Engheta, *Nat. Commun.* **2021**, *12*, 1466.
[18] F. Zangeneh-Nejad, D. L. Sounas, A. Alù, R. Fleury, *Nat. Rev. Mater.* **2021**, *6*, 207.
[19] Y. Zhang, Y. Zhang, B. Li, *Opt. Express* **2007**, *15*, 9287.
[20] Y. Fu, X. Hu, Q. Gong, *Phys. Lett. A* **2013**, *377*, 329.
[21] H. Yang, V. Khayrudinov, V. Dhaka, H. Jiang, A. Autere, H. Lipsanen, Z. Sun, H. Jussila, *Sci. Adv.* **2018**, *4*, eaar7954.
[22] H. Wei, Z. Wang, X. Tian, M. Käll, H. Xu, *Nat. Commun.* **2011**, *2*, 387.
[23] H. Wei, Z. Li, X. Tian, Z. Wang, F. Cong, N. Liu, S. Zhang, P. Nordlander, N. J. Halas, H. Xu, *Nano Lett.* **2011**, *11*, 471.
[24] J. Shamir, H. J. Caulfield, W. Micelli, R. J. Seymour, *Appl. Opt.* **1986**, *25*, 1604.
[25] Y. Zhang, Y. Wang, Y. Dai, X. Bai, X. Hu, L. Du, H. Hu, X. Yang, D. Li, Q. Dai, T. Hasan, Z. Sun, *Sci. Adv.* **2022**, *8*, eabq8246.
[26] K. S. Mohamed, *Neuromorphic Computing and Beyond*, Springer, Cham **2020**.
[27] J. Feldmann, N. Youngblood, M. Karpov, H. Gehring, X. Li, M. Stappers, M. L.e Gallo, X. Fu, A. Lukashchuk, A. S. Raja, J. Liu, C. D. Wright, A. Sebastian, T. J. Kippenberg, W. H. P. Pernice, H. Bhaskaran, *Nature* **2021**, *589*, 52.
[28] D. A. B. Miller, *Nat. Photonics* **2010**, *4*, 3.
[29] J. L. O'Brien, *Science* **2007**, *318*, 1567.
[30] N. P. de Leon, K. M. Itoh, D. Kim, K. K. Mehta, T. E. Northup, H. Paik, B. S. Palmer, N. Samarth, S. Sangtawesin, D. W. Steuerman, *Science* **2021**, *372*, 6539.
[31] A. Macho, D. Pérez, J. Capmany, *Laser Photonics Rev.* **2021**, *15*, 2000473.
[32] R. J. C. Spreeuw, *Found Phys* **1998**, *28*, 361.
[33] R. J. C. Spreeuw, *Phys. Rev. A* **2001**, *63*, 062302.
[34] L. B. Kish, Quantum computing with analog circuits: Hilbert space computing. In Proc. of SPIE 5055, Smart Structures and Materials 2003: Smart Electronics, MEMS, BioMEMS, and Nanotechnology, **2003**, 0277–786X.
[35] M. Van den Nest, Classical simulation of quantum computation, the Gottesman-Knill theorem, and slightly beyond. (Preprint) arxiv: 0811.0898, **2010**.
[36] B. R. La Cour, G. E. Ott, *New J Phys* **2015**, *17*, 053017.
[37] C. Wetterich, *Nucl. Phys. B* **2019**, *948*, 114776.
[38] S. Zhang, P. Li, B. Wang, Q. Zeng, X. Zhang, *J Phys Commun* **2019**, *3*, 015008.
[39] S. Zhang, Y. Zhang, Y. Sun, H. Sun, X. Zhang, *Opt. Express* **2019**, *27*, 436.
[40] M. Balynsky, H. Chiang, D. Gutierrez, A. Kozhevnikov, Y. Filimonov, A. Khitun, *J. Appl. Phys.* **2021**, *130*, 164903.
[41] J. I. Cirac, *Nanophotonics* **2021**, *10*, 453.
[42] C. H. Yang, R. C. C. Leon, J. C. C. Hwang, A. Saraiva, T. Tanttu, W. Huang, J. Camirand Lemyre, K. W. Chan, K. Y. Tan, F. E. Hudson, K. M. Itoh, A. Morello, M. Pioro-Ladrière, A. Laucht, A. S. Dzurak, *Nature* **2020**, *580*, 350.
[43] E. Desurvire, *Classical and Quantum Information Theory: An Introduction for the Telecom Scientist*, Cambridge University Press, Cambridge **2009**.
[44] S. M. Barnett, *Quantum Information*, Oxford University Press, Oxford **2009**.
[45] C. E. Shannon, *Bell Syst. Tech. J.* **1948**, *27*, 379.
[46] A. Borst, F. Theunissen, *Nat. Neurosci.* **1999**, *2*, 947.
[47] H. Jaeger, *Neuromorphic Comput. Eng.* **2021**, *1*, 012002.
[48] C. Weedbrook, S. Pirandola, R. G-Patrón, N. J. Cerf, T. C. Ralph, J. H. Shapiro, S. Lloyd, *Rev. Mod. Phys.* **2012**, *84*, 621.
[49] L. N. Gatti, J. Lacalle, *Quantum Inf. Process.* **2018**, *17*, 192.
[50] J. Tang, D. Bishop, S. Kim, M. Copel, T. Gokmen, T. Todorov, S. Shin, K.-T. Lee, P. Solomon, K. Chan, W. Haensch, J. Rozen, ECRAM as scalable synaptic cell for high-speed, low-power neuromorphic computing. in *IEEE International Electron Devices Meeting (IEDM)*, **2018**, 8614551.
[51] C. Cohen-Tannoudji, B. Diu, F. Laloë, *Quantum Mechanics, Vol. I: Basic Concepts, Tools, and Applications*, Wiley, Weinheim **2020**, Ch. 2.
[52] G. Landi, A. Zampini, *Linear Algebra and Analytic Geometry for Physical Sciences*, Springer, Cham **2018**.
[53] S. Popescu, *Nat. Phys.* **2014**, *10*, 264.
[54] E. Rieffel, W. Polak, *Quantum Computing: A Gentle Introduction*, The MIT Press, Massachusetts, **2011**.
[55] D. A. B. Miller, *Quantum Mechanics for Scientist and Engineers*, Cambridge University Press, **2008**.
[56] S. Roman, *Advanced Linear Algebra*, Springer, New York **2005**.
[57] B. C. Hall, *Lie Groups, Lie Algebras, and Representations. An Elementary Introduction*, Springer, New York **2003**.
[58] A. Kirillov, *An Introduction to Lie Groups and Lie Algebras*, Cambridge University Press, Cambridge **2008**.
[59] G. H. Golub, C. F. Van Loan, *Matrix Computations*, The Johns Hopkins University Press, Baltimore **2013**.
[60] M. Hamada, *R Soc Open Sci* **2014**, *1*, 140145.
[61] A. De Vos, S. De Baerdemacker, *Phys. Rev. A* **2016**, *94*, 052317.
[62] H. Führ, Z. Rzeszotnik, *Linear Algebra Appl* **2018**, *547*, 32.
[63] T. C. Ralph, N. K. Langford, T. B. Bell, A. G. White, *Phys. Rev. A* **2002**, *65*, 062324.
[64] J. Wang, F. Sciarrino, A. Laing, M. G. Thompson, *Nat. Photonics* **2020**, *14*, 273.
[65] S. Pai, B. Bartlett, O. Solgaard, D. A. B. Miller, *Phys. Rev. Appl.* **2019**, *11*, 064044.
[66] D. Pérez, A. López, P. Dasmahapatra, J. Capmany, *Nat. Commun.* **2020**, *11*, 6359.
[67] S. Bandyopadhyay, R. Harmerly, D. Englund, *Optica* **2021**, *8*, 1247.
[68] J. Zhang, B. Haq, J. O'Callaghan, A. Gocalinska, E. Pelucchi, A. J. Trindade, B. Corbett, G. Morthier, G. Roelkens, *Opt. Express* **2018**, *26*, 8821.
[69] T. Thiessen, J. C. C. Mak, J. D. Fonseca, K. Ribaud, C. Jany, J. K. S. Poon, S. Menezo, *J Lightwave Technol* **2020**, *38*, 3000.
[70] X.-D. Zhang, *A Matrix Algebra Approach to Artificial Intelligence*, Springer, Singapore **2020**.

[71] A. Fawzi, M. Balog, A. Huang, T. Hubert, B. R-Paredes, M. Barekatain, A. Novikov, F. J. R. Ruiz, J. Schrittwieser, G. Swirszcz, D. Silver, D. Hassabis, P. Kohli, *Nature* **2022**, *610*, 47.
[72] S. Rabanser, O. Shchur, S. Günnemann, Introduction to tensor decompositions and their applications in machine learning. (Preprint) arxiv: 1711.10781, **2017**.
[73] V. P. Paucaa, J. Pipera, R. J. Plemmons, *Linear Algebra Appl* **2006**, *416*, 29.
[74] A. A. Maciejewski, C. A. Klein, *Int. J. Robotics Research* **2016**, *8*, 63.
[75] H. Sun, R. F. Murphy, *Bioinformatics* **2021**, *37*, 3538.
[76] A. A. Arabi, *Future Drug Discovery* **2021**, *3*, 2.
[77] H. Iqbal, D. Campo, L. Marcenaro, D. M. Gomez, C. Regazzoni, *Signal Process.* **2021**, *188*, 108170.
[78] Q. Li, W. Cai, X. Wang, Y. Zhou, D. D. Feng, M. Chen, Medical image classification with convolutional neural network. In *13th International Conference on Control Automation Robotics & Vision (ICARCV)*, **2014**, 7064414.
[79] R. Brem, *Genome Biol.* **2000**, *1*, 0066.
[80] V. J-Jacinto, L. G-Romero, C.-F. M-Cruz, In *Pattern Recognition Techniques Applied to Biomedical Problems* (Ed.: M. Ortiz-Posadas), Springer, Cham **2020**, pp. 35–61.
[81] E. Knill, R. Laflamme, *Phys. Rev. Lett.* **1998**, *81*, 5672.
[82] R. Ghobadi, J. S. Oberoi, E. Zahedinejhad, The power of one qubit in machine learning. (Preprint) arxiv: 1905.01390, **2019**.
[83] F. Stelzer, A. Röhm, R. Vicente, I. Fischer, S. Yanchuk, *Nat. Commun.* **2021**, *12*, 5164.
[84] E. H. Bareiss, *J. Inst. Math. Appl.* **1972**, *10*, 68.
[85] A. Brandt, A. A. Lubrecht, *J Comput Phys* **1990**, *90*, 348.
[86] I. Podlubny, A. Chechkin, T. Skovranek, Y. Chen, B. M. V. Jara, *J Comput Phys* **2009**, *228*, 3137.
[87] A. Bayliss, C. I. Goldstein, E. Turkel, *J Comput Phys* **1983**, *49*, 443.
[88] Z. Baia, G. Faheya, G. Golub, *J Comput Appl Math* **1996**, *74*, 71.
[89] O. Goldreich, *Computational Complexity: A Conceptual Perspective*, Cambridge University Press, Cambridge **2008**.
[90] E. Tang, *Nat. Rev. Phys.* **2022**, *4*, 692.
[91] W. Hubbard, D. Schwartz, J. Denker, H. P. Graf, R. Howard, L. Jackel, B. Straughn, D. Tennant, *AIP Conf. Proc.* **1986**, *151*, 227.
[92] A. Van Schaik, *Neural Networks* **2001**, *14*, 617.
[93] G. Andersson, S. W. Jolin, M. Scigliuzzo, R. Borgani, M. O. Tholén, J. C. R. Hernández, V. Shumeiko, D. B. Haviland, P. Delsing, *PRX quantum* **2022**, *3*, 010312.
[94] M. Schlosshauer, *Rev. Mod. Phys.* **2005**, *76*, 1267.
[95] E. Galiffi, R. Tirole, S. Yin, H. Li, S. Vezzoli, P. A. Huidobro, M. G. Silveirinha, R. Sapienza, A. Alù, J. B. Pendry, *Photonics Time-Varying Media.* **2022**, *4*, 014002.
[96] O. Reshef, I. D. Leon, M. Z. Alam, R. W. Boyd, *Nat. Rev. Mater.* **2019**, *4*, 535.
[97] Q. Wang, E. T. F. Rogers, B. Gholipour, C.-M. Wang, G. Yuan, J. Teng, N. I. Zheludev, *Nat. Photonics* **2016**, *10*, 60.
[98] Z. Fang, R. Chen, J. Zheng, A. I. Khan, K. M. Neilson, S. J. Geiger, D. M. Callahan, M. G. Moebius, A. Saxena, M. E. Chen, C. Rios, J. Hu, E. Pop, A. Majumdar, *Nat. Nanotechnol.* **2022**, *17*, 842.
[99] T. Albash, D. A. Lidar, *Rev. Mod. Phys.* **2018**, *90*, 015002.
[100] F. Flamini, N. Spagnolo, F. Sciarrino, *Rep Prog Phys* **2019**, *82*, 016001.
[101] D. Jalas, A. Petrov, M. Eich, W. Freude, S. Fan, Z. Yu, R. Baets, M. Popović, A. Melloni, J. D. Joannopoulos, M. Vanwolleghem, C. R. Doerr, H. Renner, *Nat. Photonics* **2013**, *7*, 579.
[102] G. P. Agrawal, *Nonlinear Fiber Optics*, Elsevier, Oxford **2013**.
[103] J. R. Rausell-Campo, D. Pérez-López, *IEEE J. Sel. Top. Quantum Electron.* **2022**, *28*, 8300513.
[104] A. N. Gomez, M. Ren, R. Urtasun, R. B. Grosse, In *Advances in Neural Information Processing Systems (NIPS)*, **2017**, pp. 2211.
[105] M. MacKay, P. Vicol, J. Ba, R. Grosse, Reversible recurrent neural networks, (Preprint) arxiv: 1810.10999, **2018**.